

AWARD NUMBER: W81XWH-19-1-0168

TITLE: Quantitative assessment of post-traumatic osteoarthritis by multi-modal optical coherence tomography

PRINCIPAL INVESTIGATOR: B. Hyle Park

CONTRACTING ORGANIZATION: The Regents of the University of California

REPORT DATE: July 2020

TYPE OF REPORT: Annual

PREPARED FOR: U.S. Army Medical Research and Development Command  
Fort Detrick, Maryland 21702-5012

DISTRIBUTION STATEMENT: Approved for Public Release;  
Distribution Unlimited

The views, opinions and/or findings contained in this report are those of the author(s) and should not be construed as an official Department of the Army position, policy or decision unless so designated by other documentation.

# REPORT DOCUMENTATION PAGE

Form Approved  
OMB No. 0704-0188

Public reporting burden for this collection of information is estimated to average 1 hour per response, including the time for reviewing instructions, searching existing data sources, gathering and maintaining the data needed, and completing and reviewing this collection of information. Send comments regarding this burden estimate or any other aspect of this collection of information, including suggestions for reducing this burden to Department of Defense, Washington Headquarters Services, Directorate for Information Operations and Reports (0704-0188), 1215 Jefferson Davis Highway, Suite 1204, Arlington, VA 22202-4302. Respondents should be aware that notwithstanding any other provision of law, no person shall be subject to any penalty for failing to comply with a collection of information if it does not display a currently valid OMB control number. PLEASE DO NOT RETURN YOUR FORM TO THE ABOVE ADDRESS.

<b>1. REPORT DATE</b> July 2020		<b>2. REPORT TYPE</b> Annual		<b>3. DATES COVERED</b> 06/01/2019-05/31/2020	
<b>4. TITLE AND SUBTITLE</b> Quantitative assessment of post-traumatic osteoarthritis by multi-modal optical coherence tomography				<b>5a. CONTRACT NUMBER</b>	
				<b>5b. GRANT NUMBER</b> W81XWH-19-1-0168	
				<b>5c. PROGRAM ELEMENT NUMBER</b>	
<b>6. AUTHOR(S)</b> B. Hyle Park, Jin Nam  E-Mail: hylepark@engr.ucr.edu; jnam@engr.ucr.edu				<b>5d. PROJECT NUMBER</b>	
				<b>5e. TASK NUMBER</b>	
				<b>5f. WORK UNIT NUMBER</b>	
<b>7. PERFORMING ORGANIZATION NAME(S) AND ADDRESS(ES)</b> California, University of, Riverside 200 University Office Building Riverside, CA 92521				<b>8. PERFORMING ORGANIZATION REPORT NUMBER</b>	
<b>9. SPONSORING / MONITORING AGENCY NAME(S) AND ADDRESS(ES)</b> U.S. Army Medical Research and Development Command Fort Detrick, Maryland 21702-5012				<b>10. SPONSOR/MONITOR'S ACRONYM(S)</b>	
				<b>11. SPONSOR/MONITOR'S REPORT NUMBER(S)</b>	
<b>12. DISTRIBUTION / AVAILABILITY STATEMENT</b> Approved for Public Release; Distribution Unlimited					
<b>13. SUPPLEMENTARY NOTES</b>					
<b>14. ABSTRACT</b> Evidence from osteoarthritis (OA) studies suggests that there is a narrow time window in the early stages of the disease when cartilage can be functionally restored to reduce further degeneration. Small internal cartilage damages due to traumatic joint injuries are hard to detect with the traditional imaging technologies but pose a significant risk of inducing OA later. Our goal is to develop a non-destructive and label-free combination of optical coherence tomography (OCT) based methods for early detection of PTOA by assessment of mechanical strength, which is dependent upon both GAG and collagen, through our novel method for optical coherence elastography (OCE) based on fringe washout, and of collagen by itself through polarization-sensitive OCT. While our progress has been slowed by the current COVID-19 pandemic, we have demonstrated, for the first time to our knowledge, volumetric assessment of the mechanical properties of cartilage and bone. We anticipate successful completion of our aims as our campus re-opens for research activities. This work will provide the first optical method capable of complete non-destructive assessment of sub-surface cartilage degeneration for PTOA diagnosis.					
<b>15. SUBJECT TERMS</b> post-traumatic osteoarthritis, early detection, cartilage, glycosaminoglycan, collagen, mechanical strength, Young's modulus, optical imaging, optical coherence tomography, optical coherence elastography, polarization-sensitive					
<b>16. SECURITY CLASSIFICATION OF:</b>			<b>17. LIMITATION OF ABSTRACT</b>  Unclassified	<b>18. NUMBER OF PAGES</b>  11	<b>19a. NAME OF RESPONSIBLE PERSON</b> USAMRMC
<b>a. REPORT</b>  Unclassified	<b>b. ABSTRACT</b>  Unclassified	<b>c. THIS PAGE</b>  Unclassified			<b>19b. TELEPHONE NUMBER (include area code)</b>

## TABLE OF CONTENTS

	<u>Page</u>
1. Introduction	4
2. Keywords	4
3. Accomplishments	4
4. Impact	9
5. Changes/Problems	10
6. Products	10
7. Participants & Other Collaborating Organizations	10
8. Special Reporting Requirements	11
9. Appendices	11

## 1. INTRODUCTION

Evidence from osteoarthritis (OA) studies suggests that there is a narrow time window in the early stages of the disease when cartilage can be functionally restored to reduce further degeneration. These studies collectively demonstrate the importance of early detection of OA to enhance the effectiveness of subsequent therapies. However, current technologies, including arthroscopy, X-ray radiography, and MRI, can detect OA only after significant and irreversible damage to articular cartilage has already occurred. Small internal cartilage damages due to traumatic joint injuries are hard to detect with the traditional imaging technologies but pose a significant risk of inducing OA later. Therefore, it is essential to develop tomographic imaging tools with high resolution that can provide direct assessment of intra-cartilaginous damage in individual patients at the earliest stages of PTOA. We believe that high-resolution assessment of not only the surface, but also the interior portions of cartilage will allow for detection of OA at a much earlier time point, thus providing an opportunity to prevent the progression of or even to allow for repair of cartilage damage and to guide therapies to where they are most effective for existing damage. To take advantage of this therapeutic window, our goal is to develop a non-destructive and label-free combination of optical coherence tomography (OCT) based methods for early detection of PTOA. Cartilage damage at the early stages of OA is known to heterogeneously alter local density/mechanical properties of extracellular matrix (ECM). The mechanical properties of cartilage derive from extracellular matrix components of glycosaminoglycan (GAG) and collagen, with the density and organization of both known to change early in PTOA development. Several investigators have previously established PS-OCT as a method for quantifying localized changes in collagen, but this method is not sensitive to glycosaminoglycan (GAG), which also significantly contributes to the mechanical properties of cartilage. A smaller number of separate studies have investigated the use of optical coherence elastography (OCE) to examine the overall mechanical properties of cartilage, but these techniques cannot provide volumetric quantification in real time. Our novel method for OCE takes advantage of fringe washout, an artifact related to motion during the acquisition time of spectral domain OCT systems, and can be used to rapidly scan volumes of tissue in combination with PS-OCT. Our hypothesis is that robust and sensitive detection of early PTOA can be achieved by utilizing OCE to quantify subsurface damages in GAG loss and its associated cartilage swelling when complemented by quantification of localized changes in collagen content/disorganization with PS-OCT. This project has three aims: 1. optimize fringe washout based OCE, 2. optically quantify GAG in cartilage, and 3. identify optical signatures of cartilage degeneration in early stages of a rat PTOA model. Completion of these aims will provide the first optical method capable of complete non-destructive assessment of sub-surface cartilage degeneration for PTOA diagnosis.

## 2. KEYWORDS

post-traumatic osteoarthritis, early detection, cartilage, glycosaminoglycan, collagen  
mechanical strength, Young's modulus

optical imaging, optical coherence tomography, optical coherence elastography, polarization-sensitive

## 3. ACCOMPLISHMENTS

### What were the major goals of the project?

Specific Aim 1: optimize fringe washout based optical coherence elastography

- Major task 1: relative delay optimization
  - Milestone: autocalibration of optimized PS-OCT/OCT imaging system (month 4)
    - Progress: 100%
- Major task 2: characterization of sensitivity and resolution
  - Milestone: optimized OCE acquisition parameters based on imaging scenario with expected sensitivity and resolution based on sample size and composition (month 7)
    - Progress: 90%

Specific Aim 2: optically quantify GAG in cartilage

- Major task 1: bovine cartilage explant experimentation and analysis
  - Milestone: calibrated determination of mechanical and biochemical properties of cartilage based on optical imaging (month 10)
    - Progress: 0%

Specific Aim 3: identify optical signatures of cartilage degeneration in early stages of a rat PTOA model

- Major task 1: early rat OA model experimentation and analysis
  - Milestone: obtain ACURO approval, obtain UCR IACUC approval of protocol amendment (month 5)
    - Progress: 100%
  - Milestone: identification of early PTOA based on optical assessment of changes in cartilage (month 18)
    - Progress: 10%

**What was accomplished under these goals?**

Specific Aim 1: Hardware development – PS-OCT

Our initial plan was to continue optimizing our OCE technology for use with a PS-OCT system with a center wavelength in the 1310 nm range. However, we concluded that increased sensitivity and robustness of the ultrasound perturbation of tissue required an increased optical path length through water. In order to counter optical absorption of light through water, we decided that the best approach would be to instead keep the two systems separate, with PS-OCT imaging done in the 1310 nm range and OCE in a visible wavelength length (as there is significantly less optical absorption in the visible wavelength range).

This has allowed for significant improvements to the optical hardware in the PS-OCT system, with the primary shortcomings in the previous iteration of the system being difficulty in positioning a sample without direct visual feedback and less than optimal light coupling throughout the system. In preparation for acute imaging directly before and after induction of traumatic injury to a rat knee using the drop tower described in Aim 3, we also wanted to increase the positioning flexibility of the sample arm handpiece as well; the previous setup, while quite stable, was bolted onto the optical table and therefore required a sample to be mostly adjusted to it since only small distance and angle changes could be made to the rigid sample arm. The new sample arm was designed to be used more like a handpiece which can be positioned more flexibly with optical columns so that a greater variety of samples and sample positions can be used.

The sample arm has a custom-machined part milled from aluminum which serves to both hold an XY galvanometer (galvo) set as well as other mounting threads and holes for the rest of the sample arm’s components. The beam path is as follows: a collimated beam emerges from the collimator through a shutter which can be used to easily block the sample arm beam for reference image acquisition. The beam then interacts with the XY galvo mirrors which position the resulting collimated beam laterally. The positioned beam is then reflected down towards the lenses by a dichroic mirror. This dichroic mirror keeps laser light away from a CMOS camera on the opposite end of the sample arm to capture an image of the sample in the visual spectrum, with visual feedback provided through the camera expected to greatly facilitate gross positioning of the sample.

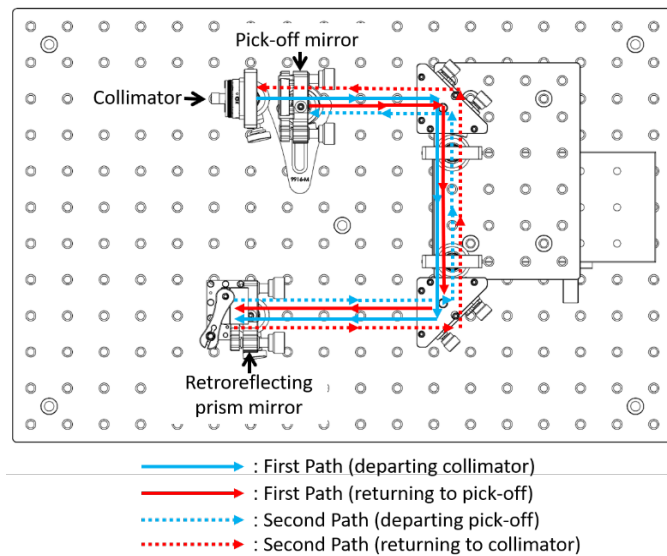


**Figure 2: schematic of the revised PS-OCT reference arm.**

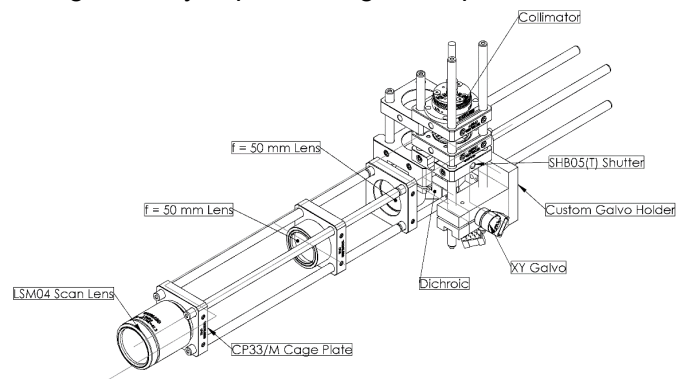


**Figure 1: schematic of the revised PS-OCT sample arm.**

To reduce image warping artifact created from galvo mirror positioning being mismatched from the focal length of the next lens used, we employ a 4f lens arrangement that allows the use of a simple tube lens with a longer focal length that allows enough physical spacing from the lens to the galvo mirror center through the dichroic. Instead of an eye’s lens at the end of the 4f, there is a scanning lens which focuses and collects light into and from the sample. To illuminate the sample for the camera, a ring light may be added to the end of the sample arm.

The increased path length in the sample arm necessitated a matching increase in the length of the reference arm. The overall beam path was revised to include a pick-off mirror such that the overall optical path

length through the reference arm is now 4x the physical length (previously 2x). This is extremely advantageous for producing a reference arm that maintains constant returned power over a long path length change because a stage with relatively short travel can be used as compared to something like a dovetail rail. This is because there is less risk of vertical or lateral shifting over the travel of a short stage versus a longer stage or rail due to manufacturing defects. Because the stage used is a single stage translated by two micrometers, the height of the reference arm components can be kept to a minimum and reference arm path length can be precisely set.

**Specific Aim 1: Hardware development – OCE**

Our OCE system to measure the ultrasound-induced variation in intensity is based on a GPU-accelerated spectral-domain OCT system with a center wavelength of 560 nm. Visible laser beam from a broadband supercontinuum source (Fianium Supercontinuum Laser SC-400-4-T, NKT Photonics, Denmark) is sent into an interferometer (a 90/10 fiber splitter) and divided into sample and reference beams with equal optical path lengths. The returning coherent optical spectrum is dispersed by a transmission grating and focused with a plano convex lens onto one line scan camera (Sprint Series Line Scan Camera spL4096-140km, Basler, Germany).

The results in our initial application were obtained after optimized acquisition with a commercial ultrasound pulser-receiver (Olympus 5077PR). While these results were promising, the maximum perturbation power on tissue was limited. We were fortunate in obtaining a customized 4.5 MHz ring ultrasound transducer designed and manufactured by Dr. Qifa Zhou’s research team at USC for pulsed tissue excitation and have been able to achieve vastly superior results. Sinusoidal signals at the resonant frequency of the transducer with a square wave modulation are generated by a function generator and amplified before being sent into the transducer. The curved piezoelectric ceramic surface of the transducer focuses the output ultrasonic impulses on the sample with an acoustic focal length of 23 mm. OCT sample arm light is focused by a 50 mm focal length doublet lens and penetrates through the center hole of the ring transducer. The acoustic and optical focuses are aligned before each experiment. A water-filled chamber was designed to accommodate the OCT imaging probe, ultrasound transducer and sample holding component.

Our fringe-washout based OCE method for real-time cross-sectional mechanical assessment of tissue involves the comparison of the backscattered optical intensity in alternating pairs of depth profiles. The amount of ultrasound-

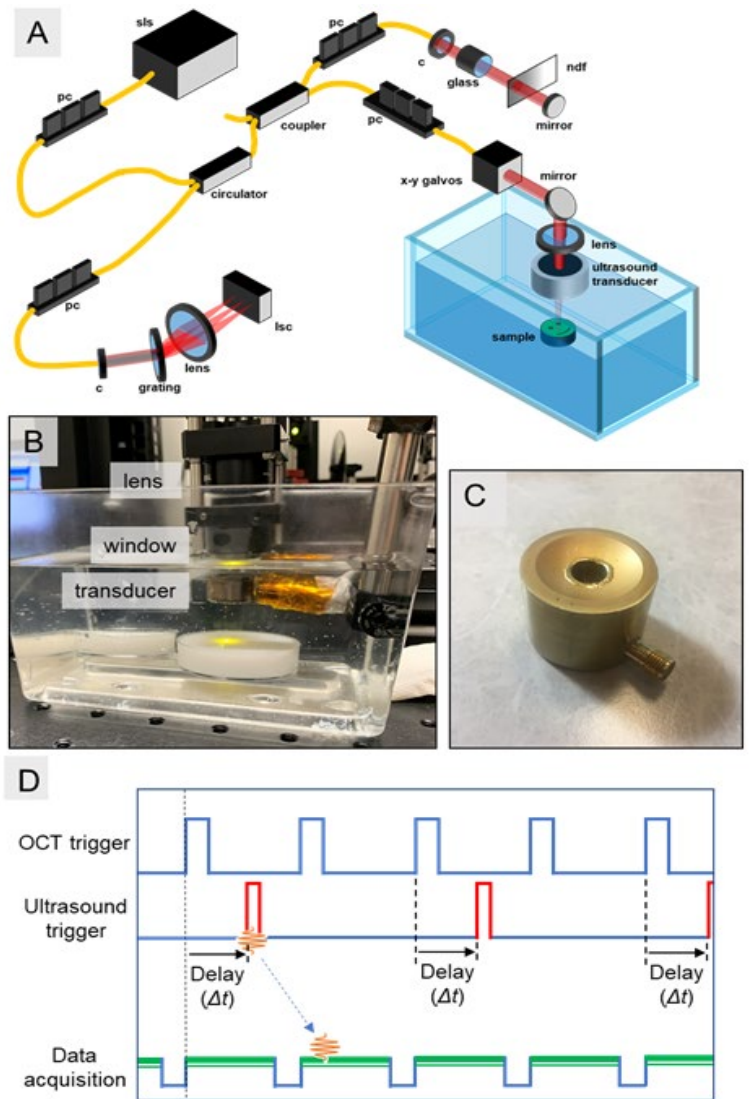


Figure 3: A) A diagram of the modified OCE system. In the sample arm, the ultrasound transducer is placed in between the lens and the sample. Scanning beam goes through the whole in the middle of the transducer to reach the sample. In the reference arm, a thick glass window is inserted for dispersion compensation. sls: supercontinuum laser source; pc: polarization controller; c: collimator; ndf: neutral density filter; lsc: line scan camera. B) The ultrasound transducer is fully immersed in water. The focuses of the lens and the transducer are axially aligned on the surface of the sample. An optical window is installed at water surface level to remove the change in reflection due to water surface vibration. C) A picture of the 4.5 MHz ring ultrasound transducer. D) A digital timing diagram of OCT-ultrasound synchronization. Ultrasound is triggered by every other line trigger signal with an option to add a time delay. A set of ultrasound acoustic waves is generated and takes certain traveling time before reaching the sample. Each line of OCT data is acquired when the data acquisition window is open (green), and the optional time delay of ultrasound triggers is set to ensure ultrasound-sample interaction occurs during the acquisition of alternating A-lines (ultrasound on).

induced fringe-washout can be determined by sending ultrasound pulses during acquisition of alternating depth profiles. Thus, it is required that ultrasound stimulation repetition frequency matches half of OCT acquisition rate. An auxiliary DAQ trigger waveform was used to synchronize ultrasound excitation with optical detection. An adjustable triggering delay mechanism ensures that the maximal tissue axial motion driven by each set of ultrasound impulses occurs during the integration of one depth profile, considering the traveling time of ultrasound propagating in water.

Specific Aim 1: System characterization and optimization – silicone phantom testing

Initial characterization of system performance and optimization of acquisition parameters was performed on silicone phantoms. Two sets of custom-built homogeneous silicone phantom with different stiffnesses (Young’s modulus is on the order of 10 kPa and 100 kPa, respectively) were fabricated

In these series of tests, the OCT line rate was set to 5 kHz and the XY-galvanometer was set to scan on a 6.0 by 6.0 mm region. Each volume of images contains information up to 1 mm in depth, and is composed of 100 frames and there are 1024 A-lines per frame. We acquired a pair of A-lines at each position, one scan as the ultrasound force is compressing the sample (ultrasound on) and the other with the sample back to stationary state (ultrasound off). The ultrasound transducer was triggered at the beginning of every other A-line scanning with no preset time delay offset. There were 90 sinusoidal cycles at 4.5 MHz in each burst of ultrasound, yielding a 20 μs period of perturbation on sample. The input voltages varied for different trials and samples.

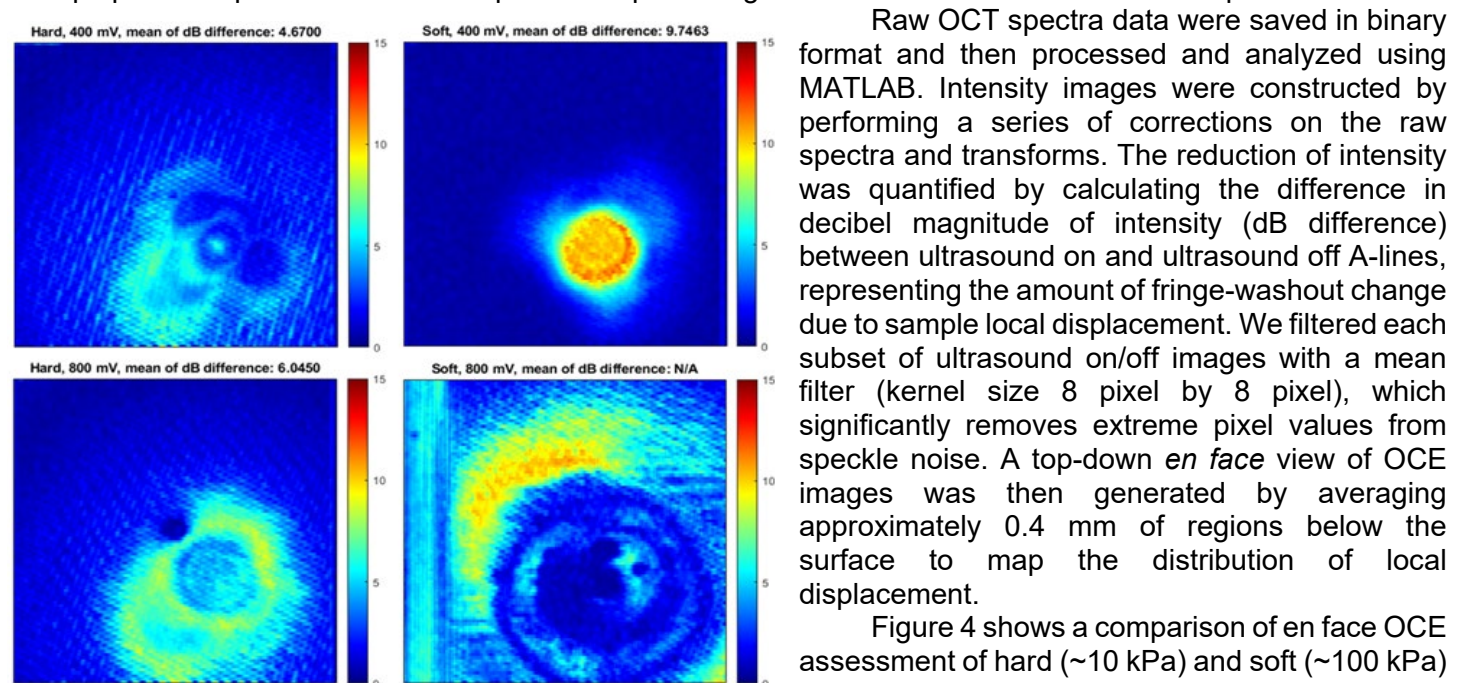


Figure 4: En face OCE images of two silicone phantom samples under different ultrasound output. Local mean dB differences are calculated by averaging the values within the ultrasound focus regions on the en face OCE images. The mean dB difference of the soft tissue under 800 mV ultrasound is not applicable because the ultrasound-driven motion is continuous over the course of the alternating A-lines scanning and exceeds the maximum of the measurable displacement.

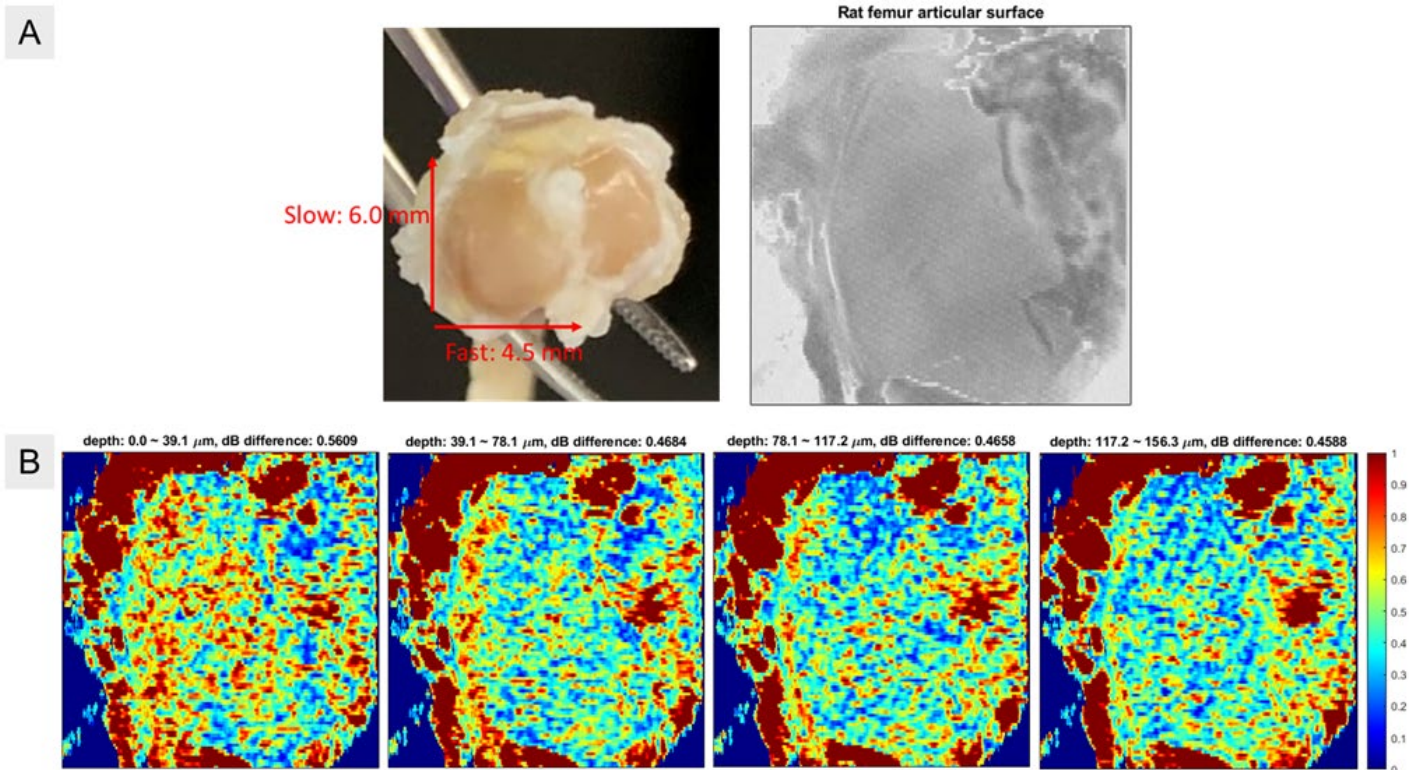
Raw OCT spectra data were saved in binary format and then processed and analyzed using MATLAB. Intensity images were constructed by performing a series of corrections on the raw spectra and transforms. The reduction of intensity was quantified by calculating the difference in decibel magnitude of intensity (dB difference) between ultrasound on and ultrasound off A-lines, representing the amount of fringe-washout change due to sample local displacement. We filtered each subset of ultrasound on/off images with a mean filter (kernel size 8 pixel by 8 pixel), which significantly removes extreme pixel values from speckle noise. A top-down *en face* view of OCE images was then generated by averaging approximately 0.4 mm of regions below the surface to map the distribution of local displacement.

Figure 4 shows a comparison of en face OCE assessment of hard (~10 kPa) and soft (~100 kPa) phantoms under 400 mV and 800 mV ultrasound input voltages. The mean of dB difference indicates the level of the ultrasound-induced reduction in intensity within the transducer focus region. Under the same ultrasonic compression power (e.g. 400 mV), the magnitude of the mean of dB difference of the soft sample is greater than that of the hard sample; while testing on the

sample, higher ultrasound power yields greater changes in intensity, as demonstrated by the OCE images of the hard sample with 400 mV and 800 mV of ultrasound pulses. These preliminary tests on phantom have validated the effectiveness of our method in assessing sample stiffness and fast mapping the distribution of local motion of the sample under certain external compression forces.

Specific Aim 1: System characterization and optimization – rat cartilage

We further validated the system by applying the same method on a fixed rat femur articular model as a mechanically heterogeneous sample to map the distribution of mechanical properties. The same ultrasound impulses with 800 mV voltage input was applied and a 6.0 mm by 4.5 mm region was imaged. Other imaging



**Figure 5: Rat femoral articular cartilage model OCE test results. A) A photo and the en face OCT intensity image of the sample. B) OCE en face images of the cartilage and bones of different layers in depth. Local mean of dB differences are calculated. The thickness of cartilage is estimated to be about 50  $\mu\text{m}$  located on the very top portion of the bone sample. The mean value of dB difference of the first layer from top (0 ~ 39.1  $\mu\text{m}$ , mostly composed of cartilage) is noticeably higher than those of the deeper regions (bone), which is consistent with the fact that cartilage is softer than bone.**

parameters remained unchanged. Since the stiffness of femoral articular cartilage is on the order of 1 MPa,<sup>1</sup> the measured dB difference value is much smaller than that of the silicone phantoms. Therefore, the color map scale was adjusted for better visualization of the elasticity information of the surface and subsurface of cartilage region. In addition, the surrounding soft tissue on the margins shows high dB difference values, which indicates much lower Young's moduli than the cartilage. It should be noted from the panels in Figure 5B, which display virtual sections of increasing depth beneath the surface of the tissue, that the variation in mechanical strength of cartilage (near the surface in the panels to the left) and the deeper bone (in the panels to the right) is evident through the decrease in dB difference. The ability to visualize this contrast demonstrates the capability of our OCE method in mapping stiffness distribution of heterogeneous biological tissue.

### Specific Aim 3: IACUC and ACURO protocol approval

A chronological listing leading to full approval of our animal use protocol is as follows:

- 07/17/2019: approval by UCR's IACUC
- 08/22/2019: all required files were received by ACURO
- 11/14/2019: we received a request for additional information
- 11/15/2019: additional information sent to ACURO
- 11/20/2019: ACURO protocol approved

### Specific Aim 3: Design and construction of drop tower

As described in our initial application, PTOA will be induced using a non-invasive drop tower method, in which various impact energies will be applied to the knees of anesthetized rats. We have completed the design and construction of the drop tower.

The rat's knee is placed on the knee support sitting on top of a load cell. A bullet-shaped indenter is held within an indenter holder which runs along two linear shafts. This ensures that the indenter strikes reliably at the

<sup>1</sup> Stolz, Martin, et al. "Early detection of aging cartilage and osteoarthritis in mice and patient samples using atomic force microscopy." *Nature nanotechnology* 4.3 (2009): 186-192.

same target location. The indenter holder contains slots and mass clamps which allow weights to be added or removed for adjusting the force of impact. Applied force may also be adjusted by the height of the indenter holder's release from the locker. The locker is held at an adjustable height with two nylon bolts pressing into the linear shafts. A quick release pin inserted perpendicularly to the linear rods allows the indenter holder to be connected to the locker and easily released from a desired height. The resulting impact force of the indenter into the knee is measured with the load cell read by a data acquisition unit (National Instruments USB-600x). Based on data from Verteramo and Seedhom,<sup>2</sup> we estimate a maximum instantaneous force to be measured of about 1962N or, with only 1g of acceleration (9.8m/s<sup>2</sup>), about 200kg. Therefore, we selected a load cell that has a maximum of 500kg. The indenter can be raised in the indenter holder up to a height about 240mm above the knee support and is designed to take up to 1kg of steel weights.

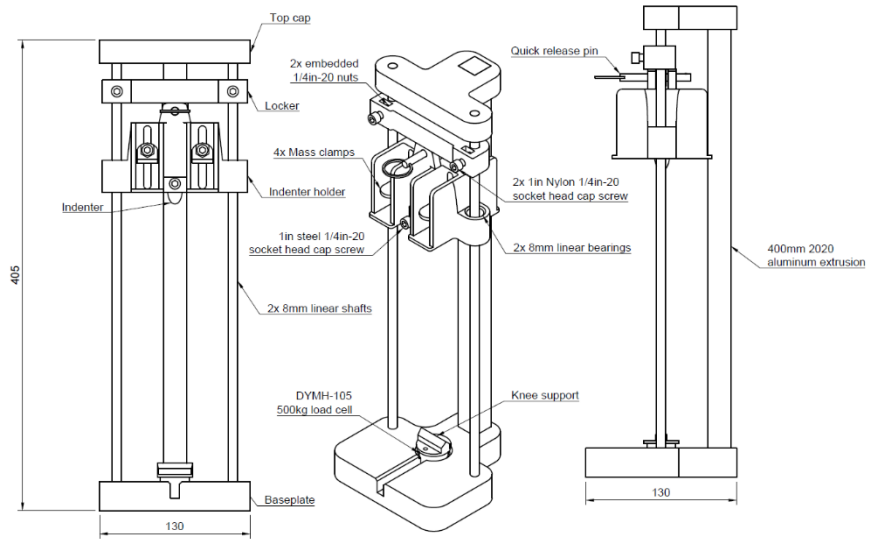


**Figure 6: schematic diagram of the drop tower, which will be used to induce PTOA in the knees of anesthetized rats.**

**What opportunities for training and professional development has this project provided?**

Nothing to report.

**How were the results disseminated to communities of interest?**

Nothing to report.

**What do you plan to during the next reporting period to accomplish the goals?**

The COVID-19 pandemic has required us to adjust the order in which portions of this project have been accomplished. Data acquisition from biological samples requires access to wet lab spaces that have largely been off-limits for the past few months. We have re-focused efforts that can be done off-campus, such as system building and data processing as described earlier in this report. UCR is currently allowing for a controlled ramp up of research activities, and we plan to complete all other portions of this project in the next reporting period. We anticipate requesting an extension of the project period to complete this work.

**4. IMPACT**

**What was the impact on the development of the principal discipline(s) of the project?**

The results shown in Figure 5 are, to the best of our knowledge, the first demonstration of volumetric OCE in bone and cartilage. Previous OCE studies<sup>3</sup> have been able to generate only single cross-sectional images of cartilage microstructure. We have been able to quantify the mechanical properties and visualize differences between bone and cartilage in a volumetric fashion. The impact of our current progress opens the possibility of non-destructive assessment of volumetric mechanical properties of bone and cartilage.

**What was the impact on other disciplines?**

Nothing to report.

<sup>2</sup> Verteramo, A; Seedhom, B. B. Effect of a single impact loading on the structure and mechanical properties of articular cartilage. *J. Biomech.* 40: 3580-3589 (2007).

<sup>3</sup> Nebelung et al. (2016). *Journal of the mechanical behavior of biomedical materials*, 56, 106-119 (2016).

Liu et al. *Quantum Electronics*, 44(8), 751 (2014).

Zaitsev et al. *Journal of biophotonics*, 12(3), e201800250 (2019).

Sovetsky et al. *Laser Physics Letters*, 15(8), 085602 (2018).

**What was the impact on technology transfer?**

Nothing to report.

**What was the impact on society beyond science and technology?**

Nothing to report.

**5. CHANGES/PROBLEMS****Changes in approach and reasons for change**

No changes to report.

**Actual or anticipated problems or delays and actions or plans to resolve them**

The COVID-19 pandemic has led to significant delays in the project; while we have not changed our overall approach, we did our best to adjust our work flow to continue to make progress under safe and socially responsible working conditions since early March. We were able to complete all aspects of the project related to hardware development and data processing as described. However, biological data acquisition was necessarily put on hold. We have continued to have weekly meetings through Zoom to continue progress overall.

In early July, UCR started allowing a controlled ramp up of research activities. We have taken advantage of the downtime to re-think and streamline our experimental workflow and are in an excellent position to resume all aspects of this project at full speed in the near future. We anticipate requesting an extension of the project period to complete the proposed work.

**Changes that had a significant impact on expenditures**

No changes to report.

**Significant changes in use or care of human subjects**

N/A.

**Significant changes in use or care of vertebrate animals**

No changes to report.

**Significant changes in use of biohazards, and/or select agents**

N/A.

**6. PRODUCTS**

Nothing to report.

**7. PARTICIPANTS & OTHER COLLABORATING ORGANIZATIONS****What individuals have worked on the project?**

Name:	B. Hyle Park
Project Role:	PI
Research Identifier:	<a href="https://orcid.org/0000-0002-0282-7162">https://orcid.org/0000-0002-0282-7162</a>
Nearest person month worked:	3
Contribution to project:	Supervision of overall project progress through weekly meetings
Name:	Jin Nam
Project Role:	PI
Research Identifier:	<a href="https://orcid.org/0000-0001-5117-8958">https://orcid.org/0000-0001-5117-8958</a>
Nearest person month worked:	3
Contribution to project:	Supervision of overall project progress through weekly meetings

Name:	Junze Liu
Project Role:	Technician
Research Identifier:	<a href="https://orcid.org/0000-0001-7946-4833">https://orcid.org/0000-0001-7946-4833</a>
Nearest person month worked:	12
Contribution to project:	Design and construction of OCE system; optimization of processing method to visualize tissue mechanical properties

Name:	Wesley Poon
Project Role:	Technician
Research Identifier:	<a href="https://orcid.org/0000-0002-9774-3673">https://orcid.org/0000-0002-9774-3673</a>
Nearest person month worked:	6
Contribution to project:	Optimization of polarization-sensitive OCT system; design and construction of drop tower

Name:	Youyi Tai
Project Role:	Graduate student
Research Identifier:	<a href="https://orcid.org/0000-0002-2530-4225">https://orcid.org/0000-0002-2530-4225</a>
Nearest person month worked:	1.5
Contribution to project:	Design and construction of drop tower; animal protocol

Name:	R.M. Imtiaz Karim Rony
Project Role:	Graduate student
Research Identifier:	<a href="https://orcid.org/0000-0002-3163-2874">https://orcid.org/0000-0002-3163-2874</a>
Nearest person month worked:	1.5
Contribution to project:	Biological sample preparation

**Has there been a change in the active other support of the PD/PI(s) or senior/key personnel since the last reporting period?**

The following are the changes to our active other support in comparison to the PCPS reported in April of 2019:

- Park: NEI U01 EY025501 has ended.
- Park: NICHD R41 HD102275 will run from 5/1/2020 through 4/31/2021.

These changes have had no impact on the effort towards this project.

**What other organization were involved as partners?**

Nothing to report.

**8. SPECIAL REPORTING REQUIREMENTS**

N/A.

**9. APPENDICES**

N/A.